Drug Development and Industrial Pharmacy, 2010; 36(7): 867–877

informa
healthcare

ORIGINAL ARTICLE

A novel pH-sensitive magnetic alginate–chitosan beads for albendazole delivery

Fa-Qin Wang[1,2], Ping Li[1], Jun-Ping Zhang[3], Ai-Qin Wang[3] and Qin Wei[1]

[1]*The Second Hospital of Lanzhou University, Lanzhou, China,* [2]*Pharmacy College of Lanzhou University, Lanzhou, China and* [3]*Lanzhou Institute of Chemical Physics, Chinese Academy of Sciences, Lanzhou, China*

Abstract

Background: Drug delivery system using polymer-coated magnetic carriers is considered as an effective strategy for passive targeting, which can not only increase drug utilization but also reduce the adverse reaction. With the carriers, sensitivity to physical stimuli (e.g., magnetic field, pH) has been developed and drugs were conjugated to form incorporating magnetic particles, so that drugs could be located to desire position. *Method*: Novel magnetic alginate (Alg)–chitosan (CS) beads loaded with albendazole (ABZ) were prepared and evaluated for pH sensitivity and drug release characteristics. The effects of six different factors (Alg concentration, the weight ratio of drug to polymer, the weight ratio of magnetite nanoparticles to polymer, $CaCl_2$ concentration, CS concentration, the volume ratio of Alg to CS) were studied on the swelling ability of the magnetic beads. The magnetic beads were characterized by Fourier transform infrared spectroscopy, scanning electron microscope, and vibrating sample magnetometry. In addition, the delivery behavior of ABZ from the magnetic beads was studied. *Result*: The magnetic Alg–CS beads had showed unique pH-dependent swelling behaviors and a continuous release of ABZ. From the magnetometer measurements data, the beads also had superparamagnetic property as well as fast magnetic response. *Conclusion*: The pH-sensitive magnetic beads may be used as a magnetic drug targeting system for ABZ in the gastrointestinal tract.

Key words: *Albendazole; chitosan; delivery properties; magnetic beads; pH-sensitive*

Introduction

Albendazole (ABZ), methyl[5-(propylthio)-1H-benzimidazol-2yl]carbamate, is a benzimidazole derivative with a broad spectrum of activity against human and animal helminthe parasites. ABZ therapy is very important in systemic cestode infection especially in inoperable or disseminated cases of hydatosis and neuro-cysticercosis[1,2]. The ABZ mode of action is through its binding to *h* tubulin and blocking of microtubule formation, leading to parasite paralysis and death[3,4]. ABZ exhibits low water solubility, but once orally administered to a host, it is metabolized into the slightly soluble sulfoxide and sulfone[5,6]. The actual bioavailability of slightly soluble sulfoxide is directly related to the short-term presence of low levels of the active metabolite in human plasma because of the limited water solubility of ABZ and its poor and erratical absorption from the gastrointestinal tract[7]. This property, which is ideal for its use against luminal infections, is a problem in the treatment of systemic helminthiasis. Furthermore, the lack of water solubility reduces flexibility for drug formulation and administration. To overcome these drawbacks, increasing the aqueous solubility of ABZ is an important goal.

Different efforts have been made to improve the detection of aqueous solubility of ABZ such as the preparation of solid dispersions[8], the use of lactose monohydrate, corn starch, polyvinylpyrrolidone, hydroxypropyl methyl cellulose and sodium lauryl sulfate[9], liposomes[10], and cyclodextrins (CDs)[11]. Numerous attempts have been made to improve its therapeutic efficacy and patient compliance. In order to reach therapeutic levels at the desired target site, large doses of drug must be administered even though only a fraction will actually reach the intended organ or disease site. Generally, ABZ appears to have serious cytotoxic effects on normal cells

Address for correspondence: Prof. Ping Li, The Second Hospital of Lanzhou University, Cuiying men Road 82, Lanzhou 730030, China. Tel: +86 931 8942043, Fax: +86 931 8463553. E-mail: gsliping@163.com

(Received 15 Nov 2009; accepted 17 Dec 2009)

ISSN 0363-9045 print/ISSN 1520-5762 online © Informa UK, Ltd.
DOI: 10.3109/03639040903567117

and tissue. Therefore, an important approach in improving the treatment effect is to better harness the potency of chemotherapeutic agents by more effectively targeting them to gastrointestinal tract, to deliver ABZ specifically into the gastrointestinal tract and to produce an effective and safe therapy for helminthiasis.

Magnetically targeted nanoparticles can be used as drug carriers to provide targeted delivery and sustained release of chemotherapeutic agents to improve bioavailability. Drugs based on carriers of core-shell magnetic nanoparticles can be easily guided to arrive at the interest position in the body by means of physical force from magnetic field (MF). Meanwhile, the outer shell (polymer layer) of the drug can effectively slow down the rate of release. Therefore, drug delivery system using polymer-coated magnetic nanoparticles is considered as an effective strategy for passive targeting, which can not only increase drug circulation but also reduce pain in patients[12]. In this regard, superparamagnetic magnetite (Fe_3O_4) nanoparticles exhibiting higher magnetization and good biocompatibility have found increasing and very promising applications in the biomedical field, such as immobilization of enzymes[13], separation of biomolecules[14], magnetic resonance imaging (MRI) contrast enhancement[15], and, particularly, drug delivery[16].

A drawback of magnetic nanoparticles for drug delivery applications is that they are most likely to be rapidly cleared by macrophages or the reticuloendothelial system before they arrive at the desired site[17]. Thus, for drug delivery applications, it is preferred that the nanoparticle drug carrier is characterized by a functionalized magnetic core and a biodegradable polymer shell. Using this approach, the possible side effects of an anticancer drug can be minimized because the drug will be covered by the polymer shell during the delivery process[18]. However, limited literatures reported the direct application of chitosan (CS)-coated magnetic nanoparticles as drug carriers.

In recent years, stimuli-responsive polymers, which can respond to external stimuli, such as pH, temperature, and electric field, have attracted a great deal of interest because of their potential applications in controlled drug delivery[19,20]. These hydrogels provide advantages over conventional therapeutic dosage forms by having higher delivery efficiency, site-specific delivery, controlled dose, and elimination or reduction of harmful side effects to the patients. By these wide advantages of the hydrogels, a number of researches have been successfully proposed to integrate active drug molecules and host materials, where to manipulate drug release desirably[21]. Recently, the use of natural polymers in the design of drug delivery formulation has received much attention. Among them, alginate (Alg) and CS are very promising and have been widely exploited in pharmaceutical industry for the controlled drug delivery[22,23].

CS, a linear polymer of D-glucosamine and *N*-acetylglucosamine units, is obtained by alkaline N-deacetylation of chitin. Because of its biodegradability, nontoxicity, and good biocompatibility, CS is a widely used polymer in tissue engineering and biomedical and pharmaceutical formulations[24,25]. To improve the CS properties for controlled drug delivery, complexation between oppositely charged molecules of Alg to prepare beads (or microspheres) that have been widely used to obtain devices for the controlled release of drugs, which can offer not only the improvement of biodegradability but also the potential of pH responsive[26]. Alg, a polyanionic copolymer of mannuronic and guluronic sugar residues, is a typical anionic polymer with carboxyl groups in the molecular chain and has been widely used in biomedical applications[27,28]. The interaction between Alg and CS and the preparation methods of Alg/CS beads had been systematically investigated[29].

Although natural polymers in the design of drug delivery formulation have evoked much interest for their superior properties, the property of drug carrier composed of homogenous material was not satisfied. Recently, composite materials as drug carrier can obtain multifunction and high-powered magnetic beads or microsphere. Therefore, a combination of Alg, CS, and magnetic particles is a potential approach to prepare magnetic beads that can be applied as a drug delivery system.

On the basis of our previous work on CS/Alg hydrogel beads for nifedipine delivery[30], this work presents magnetic Alg–CS beads for the controlled release of ABZ. Its stimulus–response property is advantageous for drug-targeting system. The magnetic beads could be located by a powerful MF in the target site where the parasites live and could be retained in the intestines with prolonged time. pH change of the environment could control the amount of drug release. Some successful applications of magnetic targeting system are achieved, However, the properties of pH-sensitive magnetic hydrogel, especially the site-specific release under the gastrointestinal condition, have not been sufficiently studied[31].

In this study, the magnetic beads were mainly focused on single calcium cross-linking, such as magnetic CS-coating Alg calcium beads, which were endowed with bioadhesion. The inner core of calcium–Alg network is coated with an Alg–CS membrane, which itself is surrounded by a layer of CS. The aim of this study was to investigate the influence of CS coating on drug release properties of the magnetic calcium–Alg beads and magnetic property of the magnetic calcium–Alg beads. Factors influencing swelling characteristics of the hydrogels were investigated and release properties of ABZ from the beads in phosphate buffer solutions of various pH (2.5, 5.0, 6.8, 7.4, and 8.0) were also studied. The results were analyzed using a semiempirical equation to reveal the drug release mechanism.

Materials and methods

Materials

CS (molecular weight is 7.5×10^5, degree of deacetylation is 80%) was acquired from Lanzhou Institute of Chemical Physics, Chinese Academy of Sciences (Lanzhou, China). Sodium alginate of low viscosity (0.02 Pa·S) for a 1% solution at 20°C was purchased from Shanghai Chemical Co., Ltd. (China). Fe_3O_4 (average size is 20 nm) was purchased from Nanjing Emperor Nano Material Co., Ltd. (Nanjing, China). Polyethylene glycol (PEG) 4000 was purchased from Tianjin Tiancheng Pharmaceutical Co., Ltd. (Tianjin, China). ABZ (purity 99.34%) was purchased from Wuhan Kanglong Century Technology Development Co., Ltd. (Wuhan, China). All other chemicals and reagents used were of analytical grade.

Single-factor design experiments

Magnetic Alg/CS beads were prepared based on the single-factor design. The independent variables are Alg concentration (X_1), the weight ratio of drug to polymer (X_2), the weight ratio of nanoparticles to polymer (X_3), $CaCl_2$ concentration (X_4), CS concentration (X_5), and the volume ratio of Alg to CS (X_6) (Table 1). On the contrary, encapsulation efficiency and loading efficiency are the response parameters as the dependent variables.

Preparation of magnetic Alg–CS beads

PEG aqueous solution (5%, w/v) was prepared by expanding 2.5 g of PEG in 50 mL of deionized water. A stock solution were prepared though adding 5 g of Fe_3O_4 into 50 mL PEG aqueous solution (5%, w/v) and was sonicated for 2 hours for the subsequent experiments.

Alg solution (2.5%, w/v) was prepared by dissolving 2.5 g of sodium Alg in 100 mL of deionized water. CS solution (2.0%, w/v) was prepared by dissolving 2.0 g of CS in 100 mL 1% acetic acid solution. The magnetic calcium–Alg beads were prepared by ionic polymerization according to the following steps: 10 mL 2.5% Alg solution (w/v), 1.25 mL stock solution of magnetite nanoparticles was mixed adequately and sonicated for 2 hours. The resulting suspension was then added dropwise in a gently stirred calcium bath (40 mL, 2.5%) for 30 minutes at a constant speed (4 mL/min). The speed has been chosen to avoid the sedimentation of ABZ particles in the syringe during the time of the beads preparation. An optimal drop height of 5 cm was used to obtain spherical beads. The wet magnetic calcium–Alg beads were transferred into CS solution and kept for 30 minutes under gentle magnetic stirring. The resulting magnetic Alg–CS beads were collected and rinsed with deionized water and dried in air overnight.

Preparation of ABZ-loaded magnetic beads

62.5 mg of ABZ was dispersed in 10 mL solution containing 2.5% sodium Alg, and then the other processes were the same as the preparation of the beads as shown earlier.

Scanning electron microscopy

Micrographs of the samples were taken using a scanning electron microscope (SEM) (JEOL, JSM-6380LV, Akishima, Tokyo, Japan). Before the observation, all samples were mounted on aluminum stubs, using double-sided adhesive tape, then hydrogel samples were coated with gold, and scanned at an accelerating voltage of 15 kV.

Table 1. Formulation of the magnetic alginate–chitosan beads utilizing single-factor design.

Formulation	X_1 (%,w/v)	X_2 (w/w)	X_3 (w/w)	X_4 (%,w/v)	X_5 (%,w/v)	X_6 (v/v)	Encapsulation efficiency (%)	Loading efficiency (%)
A1	1.5	1:3	1:1	2.0	1.0	1:3	91.48	13.66
A2	2.0	1:3	1:1	2.0	1.0	1:3	90.10	12.99
A3	2.5	1:3	1:1	2.0	1.0	1:3	96.72	13.66
B1	2.5	1:4	1:1	2.0	1.0	1:3	88.56	10.28
B2	2.5	1:5	1:1	2.0	1.0	1:3	89.00	8.50
C1	2.5	1:4	1:2	2.0	1.0	1:3	84.67	13.14
C2	2.5	1:4	1:3	2.0	1.0	1:3	79.80	13.45
D1	2.5	1:4	1:2	1.5	1.0	1:3	84.7	29.49
D2	2.5	1:4	1:2	2.5	1.0	1:3	87.59	9.66
E1	2.5	1:4	1:2	2.5	0.5	1:3	85.37	9.96
E2	2.5	1:4	1:2	2.5	1.5	1:3	87.12	9.97
E3	2.5	1:4	1:2	2.5	2.0	1:3	88.38	10.23
F1	2.5	1:4	1:2	2.5	2.0	1:4	87.69	9.86
F2	2.5	1:4	1:2	2.5	2.0	1:5	82.50	9.32

Fourier transform infrared spectroscopy

Individual beads were crushed with pestle in an agate mortar and the crushed material was mixed with potassium bromide in 1:100 proportions. The mixture was compressed to a 1 mm semitransparent disk by applying a pressure of 20 MPa (FW-4A pelleter) for 5 minutes. The Fourier transform infrared (FTIR) spectra over the wavelength range 4000–400 cm^{-1} were recorded using an FTIR spectrometer (Thermo Nicolet Nexus, TM, Madison, WI, USA).

Swelling studies

Swelling characteristics of the beads were determined by immersing dried test beads in two aqueous media: simulated gastric fluid (SGF, pH 1.5) and phosphate buffer solutions (pH 6.8) prepared according to the Chinese Pharmacopoeia 2005 at 37°C. Accurately weighed amounts of beads (ranging from 20 to 25 mg) were immersed in 20 mL media solution and the beads were removed from the swelling medium at specific time intervals. They were blotted with filter paper to absorb water on the surface and then weighed using electronic microbalance (Model NE2155; Genius, Goettingen, Germany) immediately. Swelling ratio (SR) of the sample was calculated according to the following expression[32, 33]:

$$\mathrm{SR} = \frac{W - W_0}{W_0}, \tag{1}$$

where W is the weight of the swollen beads and W_0 is the initial weight of the beads.

Assay of drug content

The beads containing ABZ (10 mg) were pulverized and incubated in 25 mL citrate sodium solution (5%, w/v) with a water bath at 40°C for 30 minutes, then the supernatant was extracted by ethyl acetate three times (10, 10, 10 mL), and the residue was dissolved in glacial acetic acid after evaporation of ethyl acetate. The whole mixture was transferred into a 25-mL volumetric flask, added methanol to scale, the resulting solution was diluted with methanol five times, then it was filtrated, the filtrate was assayed by a UV spectrophotometer at 295 nm (UV-2401PC, Shimadzu, Japan). All the experiments were carried out in triplicate.

$$\text{Loading efficiency}(\%) = \frac{W_a}{W_t} \times 100, \tag{2}$$

where W_a is the actual ABZ content and W_t is the theoretical ABZ content.

Magnetic property

A vibrating sample magnetometer (VSM) (Lake Shore, 735 VSM, Model 7304, USA) was used at room temperature to characterize the magnetic properties of pure Fe_3O_4 nanoparticles and magnetic Alg–CS beads.

In vitro drug release

The in vitro ABZ release properties from the beads were determined as follows: 0.20–0.25 g ABZ-loaded magnetic hydrogel beads were suspended in 500 mL solution and maintained at 37 ± 0.5°C under 100 rpm. The solutions were phosphate buffer solutions of various pH (2.5, 5.0, 6.8, 7.4, and 8.0). At predetermined time intervals, 2.5 mL solution was withdrawn and the dissolution medium was supplied with 2.5 mL fresh buffer solution to maintain the total volume. The drug release percent was determined as follows: the sample was extracted by ethyl acetate for 3 times (1, 1, 1 mL) and the residue was dissolved in glacial acetic acid after evaporation of ethyl acetate. The whole mixture was transferred into a 10-mL volumetric flask, added methanol to scale, and assayed spectrophotometrically at 295 nm. The drug release percent was determined using Equation (3). All samples were analyzed in triplicate.

$$\text{Drug release}(\%) = \frac{R_t}{L} \times 100, \tag{3}$$

where L and R_t represent the initial amount of drug loaded and cumulative amount of drug released at time t.

Release kinetics

The mathematical models Higuchi $M_t/M_\infty = kt^{1/2}$ equations were fitted to individual dissolution data with linear regression by SPSS 11.0 for Windows[34]. The drug release mechanisms of hydrogel beads were described by a semiempirical equation.

Statistical analysis

Statistical analysis for the determination of differences in the swelling characteristics within groups was accomplished using one-way analysis of variance, performed with a statistical program (SPSS 11.0 for Windows). For all statistical calculations, the level of significance was set at 0.05.

Results and discussion

Morphology of the beads

Morphological study of magnetic Alg–CS beads is shown in Figure 1. The wet beads had rather regular spherical shape and smooth surface at higher Alg concentration (2.5%), the diameter was about 2.5–3.5 mm (Figure 1a). As the Alg concentration increased, the beads had more spherical shape and smooth surface. In the case of dried magnetic beads, the test beads usually retained their spherical shape but showed a rather rough surface and collapsed center. The diameter was found to be 1 mm approximately (Figure 1b). SEM micrographs of dry magnetic Alg–CS beads are shown in Figure 1c–f. Detailed examination of the surface structure revealed cracks and severe wrinkles caused by partial collapsing of the polymer network during dehydration.

The wet magnetic beads are found to be spherical and dark brown because of the presence of magnetite nanoparticles and the beads can be easily removed from the aqueous solution with an MF. A creased exterior surface was observed different from the smooth and regular surface of pure Alg–CS beads. This aspect is associated with the presence of inorganic fillers[35]. It was reported that Alg–CS-coated beads usually had a heterogeneous structure with CS–Alg surface layer and calcium–Alg core, which resulted in the collapse of beads during the drying process[36].

The hydrogel beads were formed as a result of polyelectrolyte complex membrane forming through ionic interaction between $-NH^{3+}$ of CS and $-COO^{-}$ groups of Alg, giving a skin layer of membrane. The inner core of calcium–Alg network with a large amount of Fe_3O_4 nanoparticles is coated with an Alg–CS membrane, which itself is surrounded by a layer of CS[37].

FTIR spectroscopy

FTIR spectra of CS, sodium alginate, magnetic Alg–CS blank beads, magnetic Alg–CS beads containing ABZ are shown in Figure 2. The FTIR spectrum of CS showed a weak band of –OH stretching at 2877 cm^{-1}, the absorption band of the carbonyl (C=O) stretching of the secondary amide (amide I band) at 1655 cm^{-1}, and the bending vibrations of the N–H (N-acetylated residues, amide II band) at 1598 cm^{-1}[38]. The peaks at 1423 and 1381 cm^{-1} belong to the N–H stretching of the amide and ether bonds and N–H stretching (amide III band), respectively. The peaks observed at 1095 and 1033 cm^{-1} were the secondary hydroxyl group (characteristic peak of –CH–OH in cyclic alcohols, C–O stretch) and the primary hydroxyl group (characteristic peak of $-CH_2-OH$ in primary alcohols, C–O stretch)[39]. Sodium alginate showed the following distinct peaks: (1) strong absorption bands at 1626 and 1427 cm^{-1} because of carboxyl anions (asymmetric and symmetric stretching vibrations) and (2) the bridge oxygen (C–O–C, cyclic ether) stretching bands at 1029 cm^{-1} were observed as well. For the magnetic Alg–CS blank beads, the peaks observed at 1609, 1416, 1094, and 1032 cm^{-1} were the characteristic absorption band of CS and Alg; the absorption band at 1598 cm^{-1} of CS shifts to 1609 cm^{-1} after the reaction with Alg, the stretching vibration of –OH and $-NH_2$ at 3444 cm^{-1} shifts to 3420 cm^{-1} and comes broad, indicating that the polyelectrolyte complexes are formed and enhanced between CS and Alg. The characteristic absorption peak of magnetite Fe_3O_4 also appears at around 561 cm^{-1}.

The FTIR spectra of ABZ show the –NH, $-CH_3$, C=O, and amide stretching frequencies at 3331, 2957, 1712, and 1634 cm^{-1}, respectively[40], whereas those appearing at 1588, 1524 cm^{-1} are because of aromatic C=C stretching vibrations. The N–H bending vibrations are

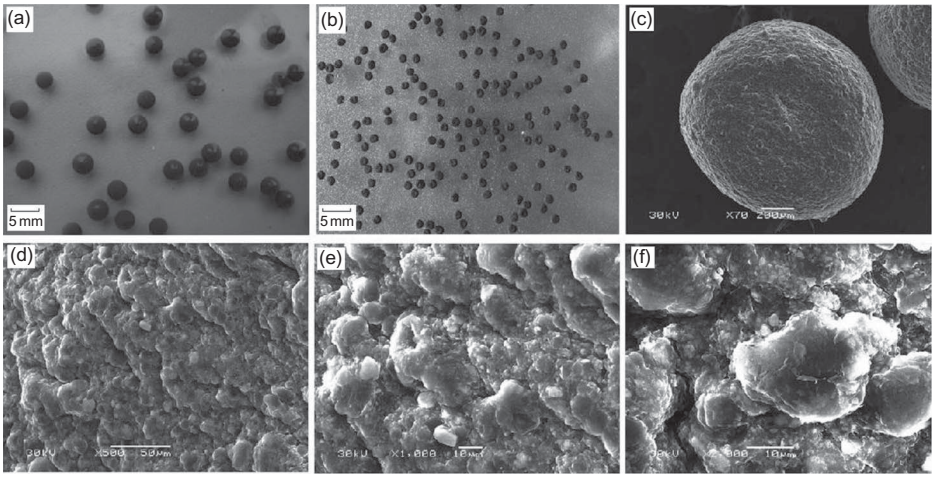

Figure 1. Photographs of magnetic alginate–CS beads: (a) wet beads; (b) dried beads. SEM micrographs of the surface morphology of magnetic alginate–CS beads: magnification ($c \times 70$), ($d \times 500$), ($e \times 1000$), ($f \times 2000$).

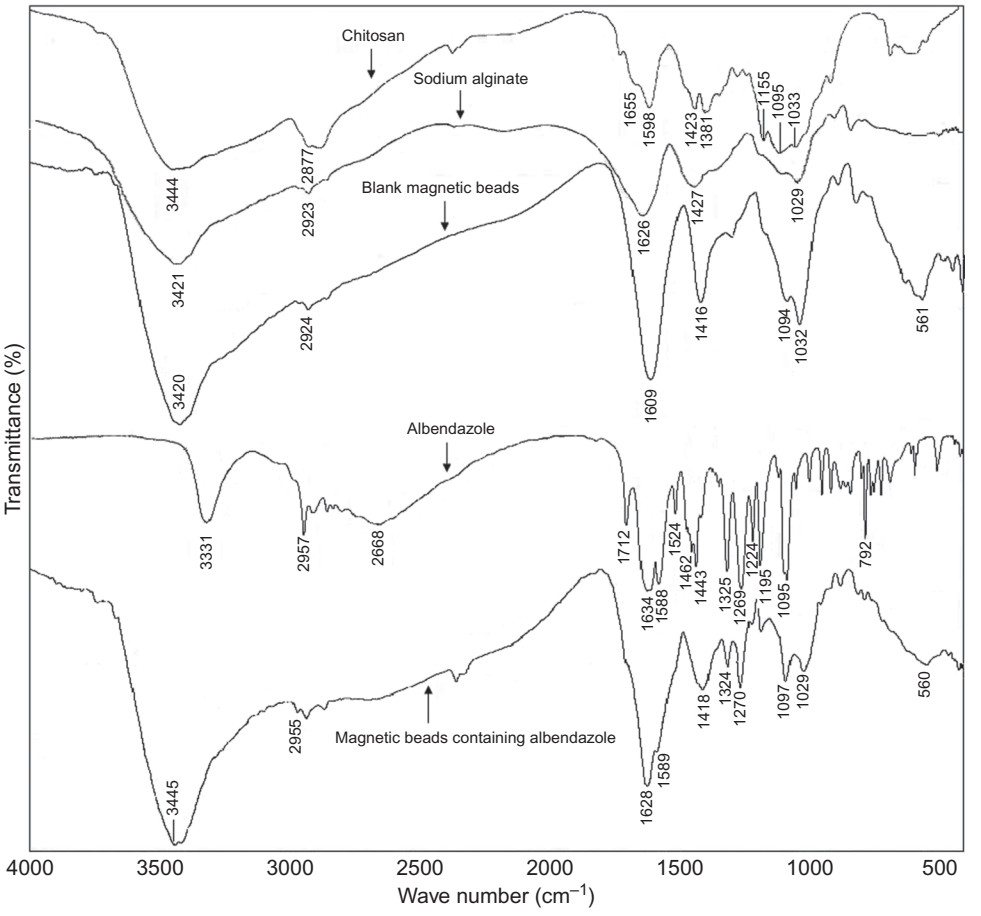

Figure 2. The FTIR spectra of CS, sodium alginate, magnetic alginate–CS blank beads, and magnetic alginate–CS beads containing ABZ.

seen at 1503 cm^{-1}. Bands at 1095 cm^{-1} are because of C–N stretching vibrations, whereas the one appeared at 1271 cm^{-1} is because of aromatic C–O stretching vibrations. The peaks at 2955, 1628, 1324, 1270, 1097 cm^{-1} were observed in the FTIR spectra of magnetic Alg–CS beads containing ABZ as well, which indicated that the chemical stability of ABZ was physically filled in the polymeric network.

Swelling characteristics of magnetic Alg–CS beads

The SRs of magnetic Alg–CS beads at pH 1.5 had no distinct difference ($P > 0.05$) among all the factors investigated except the weight ratio of magnetite nanoparticles to polymer. So, the figures of the SRs of test beads at pH 1.5 were not shown.

Figure 3 shows the swelling characteristics of magnetic Alg–CS beads at various Alg concentrations. At pH 6.8, the SRs of test beads increased significantly compared with those at pH 1.5. As the Alg concentration increased, the SR of the test beads decreased. It was found that the test beads (Alg concentration = 2.5%) had better swelling characteristics among all studied groups

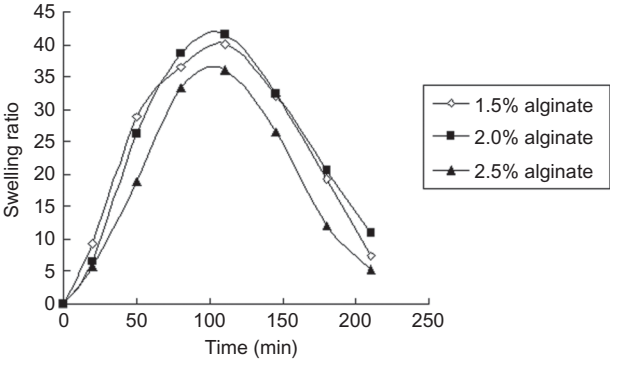

Figure 3. The influence of alginate concentration on the swelling characteristic from magnetic alginate–CS beads (the weight ratio of drug to polymer, 1/3; the weight ratio of magnetite nanoparticles to polymer to polymer, 1/1; $CaCl_2$ concentration, 2%; CS concentration, 1%; the volume ratio of alginate to CS, 1/3).

(~0.66 at pH 1.5 and ~36.2 at pH 6.8). The low-swelling degree may retain drug better at the lower end of the gastric pH range.

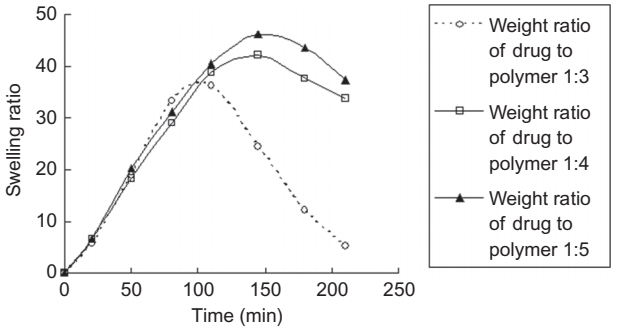

Figure 4. The influence of weight ratio of drug to polymer on the swelling characteristic from magnetic alginate–CS beads (alginate concentration, 2.5%; the weight ratio of magnetite nanoparticles to polymer, 1/1; $CaCl_2$ concentration, 2%; CS concentration, 1%; the volume ratio of alginate to CS, 1/3).

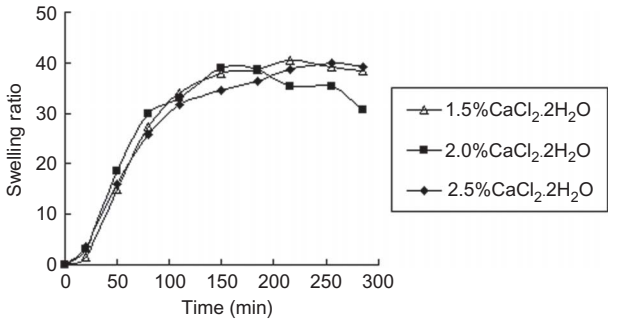

Figure 6. The influence of $CaCl_2$ concentration on the swelling characteristic from magnetic alginate–CS beads (alginate concentration, 2.5%; the weight ratio of drug to polymer, 1/4; the weight ratio of magnetite nanoparticles to polymer, 1/2; CS concentration, 1%; the volume ratio of alginate to CS, 1/3).

The weight ratio of drug to polymer is another important factor influencing the swelling characteristic besides the Alg concentration. As Figure 4 shows, the SR of test beads to the weight ratio of drug to polymer of 1/3 was lower than the other two groups at pH 6.8 and the beads eroded quickly. This phenomenon would result in a drug burst release at pH 6.8 and the hydrogel beads could not become a potential polymer carrier for the controlled release of ABZ. With increasing polymer weight, the SR of test beads increased, but the test beads eroded slowly. The SR was approximately 0.6 at pH 1.5 and 42.1 at pH 6.8 when the weight ratio of drug to polymer was 1:4. The beads may retain drug longer at pH 6.8. Therefore, the higher the weight ratio of drug to polymer, the higher the loading efficiency and the better the swelling behavior.

Figure 5 shows the effect of magnetite nanoparticles to polymer on the swelling characteristic. As shown, the SR of test beads with weight ratio of magnetite nanoparticles to polymer of 1:1 was lower than the other two groups at pH 6.8 and 1.5 ($P < 0.05$). At pH 6.8, with increasing polymer weight, the SR of test beads increased significantly. So, among all the factors investigated, the weight ratio of magnetite nanoparticles to polymer had the most influence on the swelling characteristic.

Figure 6 shows the swelling curves of magnetic Alg–CS beads prepared at different concentrations of $CaCl_2$. The SRs of all test groups had no distinct difference ($P > 0.05$) at pH 1.5 and 6.8, respectively. The SR of test beads with a 2.5% $CaCl_2$ concentration was lower than the other groups at pH 1.5. At pH 6.8, groups of 1.5%, 2.0%, and 3.0% $CaCl_2$ showed no statistical difference ($P > 0.05$), indicating that the carboxyl groups of Alg are limited. When the $CaCl_2$ concentration increased to a certain extent, the ionic cross-linking of Alg with Ca^{2+} was completed, the swelling of beads was not obviously.

Figure 7 shows the effect of CS concentration on the swelling characteristic. The SRs of all test groups had no distinct difference ($P > 0.05$) at pH 1.5 and 6.8, respectively. At pH 1.5, with increasing CS concentration, the

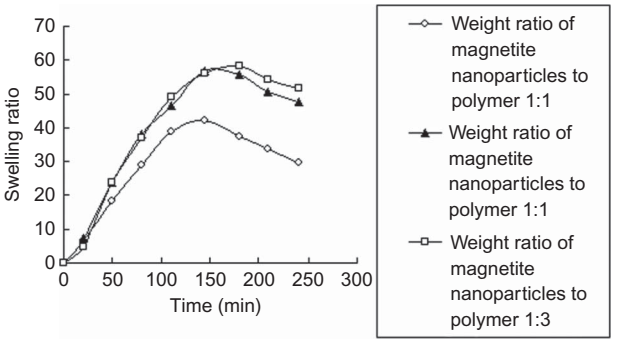

Figure 5. The influence of weight ratio of magnetite nanoparticles to polymer on the swelling characteristic from magnetic alginate–CS beads (alginate concentration, 2.5%; the weight ratio of drug to polymer, 1/4; $CaCl_2$ concentration, 2%; CS concentration, 1%; the volume ratio of alginate to CS, 1/3).

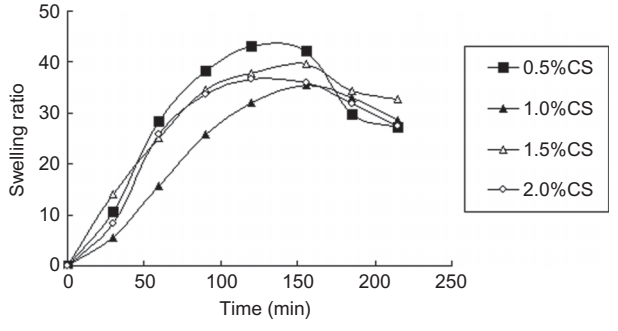

Figure 7. The influence of CS concentration on the swelling characteristic from magnetic alginate–CS beads (alginate concentration, 2.5%; the weight ratio of drug to polymer, 1/4; the weight ratio of magnetite nanoparticles to polymer, 1/2; $CaCl_2$ concentration, 2.5%; the volume ratio of alginate to CS, 1/3).

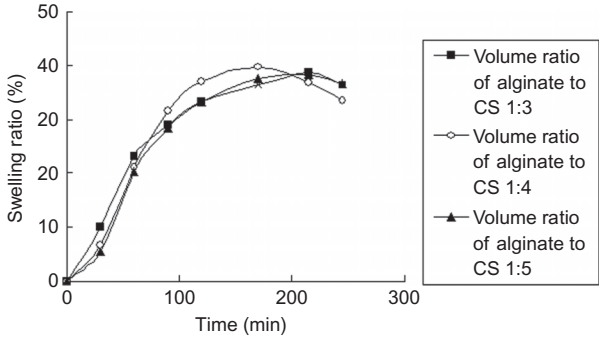

Figure 8. The influence of volume ratio of alginate to CS on the swelling characteristic from magnetic alginate–CS beads (alginate concentration, 2.5%; the weight ratio of drug to polymer, 1/4; the weight ratio of magnetite nanoparticles to polymer, 1/2; $CaCl_2$ concentration, 2.5%; CS concentration, 2%).

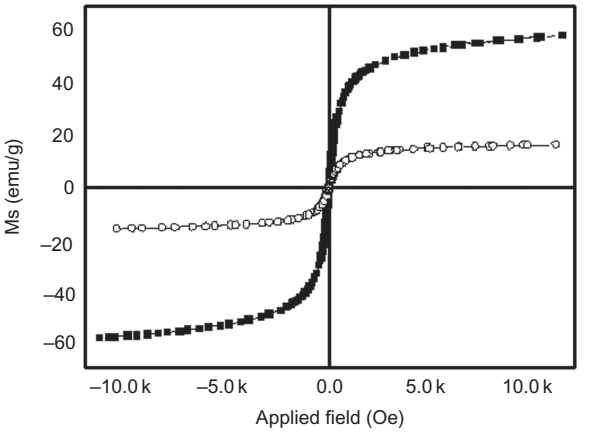

Figure 9. Magnetization curve of magnetic Alg–CS beads: magnetic alginate–CS beads containing ABZ, ◇; pure Fe_3O_4, ■.

SR of test beads decreased. It was found that the test beads (CS concentration = 2.0%) had a better swelling characteristic among all studied groups (~0.61 at pH 1.5 and ~36.2 at pH 6.8).

Figure 8 shows the influence of volume ratio of Alg to CS on the swelling characteristic from magnetic Alg–CS beads. The SRs of all test groups had no distinct difference ($P > 0.05$) at pH 1.5 and 6.8, respectively. Among all the factors investigated, the volume ratio of Alg to CS had the least influence on the swelling characteristic.

At pH 1.5, CS and Alg are partly ionized. The swelling degree of the beads was limited due to the formation of polyelectrolyte complex between $-COO^-$ groups of alginate and $-NH_3^+$ groups of CS. At this pH, the beads reached to their maximum swelling degree within 30 minutes and then shrunk gradually toward their equilibrium state. At pH 6.8, the swelling behavior of the dry beads is mainly attributed to the hydration of the hydrophilic groups of Alg and CS[41]. In this case, free water penetrates inside the beads to fill the inert pores among the polymer chains, contributing to a greater swelling degree. The SRs of test beads increased significantly because of the exchange of Ca^{2+} with Na^+, and the decrease of CS ionization, increase of ionization of the carboxyl groups of Alg, resulting in the lower binding of CS with Alg leading to less stable beads[42]. The swelling degree of beads reached to a maximum and then decreased because of disintegration and erosion of hydrogel network.

Magnetic property

Figure 9 shows a typical magnetization curve of magnetic Alg–CS beads. The saturation magnetization (σs) of the magnetic Alg–CS beads was about 15 emu/g, which comparing the reference value for the pure magnetite nanoparticles of σs was 58.57 emu/g.

Magnetic response property of the beads was determined by dispersing dried test beads in 0.2% Tween-80 solution (w/v) adequately. A given MF of about 3200 Oe was used to determine magnetic response time of the beads. When the weight ratio of magnetite nanoparticles to polymer increased, response time of the beads to MF decreased quickly. After increasing weight ratio of magnetite nanoparticles to polymer from 1:3 to 1:2, response time of the beads to MF was decreased from 9 to 2.5 seconds. Therefore, the higher the weight ratio of magnetite nanoparticles to polymer, the shorter the response time and the better magnetic response property.

The superparamagnetic property of polymer magnetic beads is critical for their application in biomedical and bioengineering fields, which prevents polymer magnetic beads from aggregation and enables them to redisperse rapidly when the MF is removed. As could be seen from Figure 4, the hysteresis loop showed superparamagnetic property (i.e., no remanence effect), indicating that the single-domain magnetic nanoparticles remained in these polymer nanoparticles.

In vitro release properties of ABZ

Figure 10 shows ABZ release profiles of the magnetic beads at various pHs at 37 ± 0.5°C as a function of time. It can be seen that the percentage released increased with the pH of the medium. Within 2 hours, the amount of ABZ released from the magnetic beads was 2.16% at pH 2.5, 29.06% at pH 5.0, 58.67% at pH 6.8, and 68.62% at pH 7.4. This suggests that the drug release properties of magnetic Alg–CS beads are pH-sensitive. Within 16 hours, ABZ release from the magnetic beads was 92.86% at pH 6.8, 94.72% at pH 7.4, whereas the amount of ABZ released from the

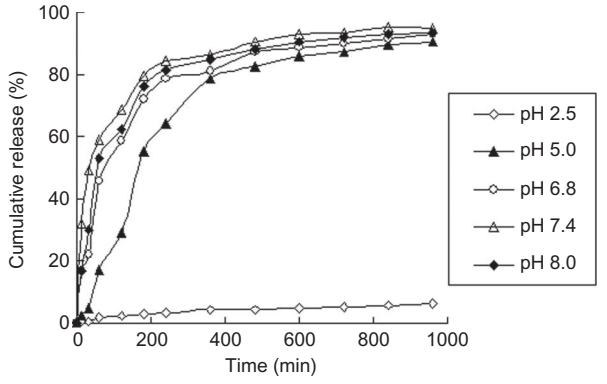

Figure 10. The cumulative release profiles of magnetic alginate–CS beads containing ABZ at various pH of media at 37°C ± 0.5°C (pH 2.5, ◇), (pH 5.0, ▲), (pH 6.8, ○), (pH 7.4, △), (pH 8.0, □). Values are mean–SD, $n = 3$.

magnetic beads was the lowest (6.12%) at pH 2.5. The release rate of ABZ from magnetic Alg–CS beads at pH 6.8 is higher than that at pH 2.5 and pH-dependent release of ABZ. The relatively low amount of ABZ released from the magnetic beads was probably related to the comparatively low degree swelling of the hydrogel at pH 2.5 (Figure 3). At pH 6.8, the amount of ABZ released increased significantly compared with those released at pH 2.5, because the swelling of the hydrogel network increased considerably because of the lower binding between the amino groups of CS and the carboxyl groups of Alg at neutral pH.

Drug release kinetics

The usage of mathematical models when designing new pharmaceutical formulations as well as for the analysis of the experimental results is essential. The Korsmeyer–Peppas equation (see below) is often used to describe the drug release behavior from polymeric systems when the mechanism is not well known or when more than one type of release phenomena are involved. This equation was used to explain the drug release mechanism and to compare the release profiles, the drug released amount versus time was used.

$$\frac{M_t}{M_\infty} = k_1 t^n \quad \text{or} \quad \log\left(\frac{M_t}{M_\infty}\right) = \log k_1 + n \log t, \qquad (4)$$

where M_t/M_∞ is the fractional amount of the drug released at time t, n is a diffusion exponent that indicates the release mechanism, and k_1 is a characteristic constant of the system. From the slope and intercept of the plot of $\log(M_t/M_\infty)$ versus $\log t$, kinetic parameters n and k_1 were calculated. For spheres, values of n between 0.43 and 0.85 are an indication of both diffusion-controlled drug release and swelling-controlled drug release (anomalous transport). Values above 0.85 indicate case-II transport that relate to polymer relaxation during gel swelling. Values below 0.43 indicate that drug release from polymer was due to Fickian diffusion[43,44].

Table 2. Estimated parameters and drug release mechanism of alginate–chitosan magnetic beads at different pH.

pH	n	k	r	Drug transport mechanism
2.5	0.6151	0.6239	0.9705	Anomalous transport
5.0	0.8360	0.5346	0.9329	Anomalous transport
6.8	0.3862	1.5307	0.9169	Fickian diffusion
7.4	0.2245	9.4254	0.9460	Fickian diffusion
8.0	0.3569	9.6984	0.9034	Fickian diffusion

Kinetic constants (k), diffusional exponents (n), and correlation coefficients (r), by linear regression of $\log(M_t/M_\infty)$ versus $\log t$; k is the constant related to the structural and geometric characteristic of the device; n is the diffusional exponents, indicative of the drug release mechanism.

ABZ-release kinetics from Alg–CS magnetic beads at different pH was shown in Table 2. ABZ release profile changes showed the drug undergoing immediate release within the first 2 hours. After 2 hours, the remaining drug is released almost linearly at pH 6.8 and 7.4. Figure 10 also shows how the drug was released in the first 2 hours. At pH 2.5–5.0, the release was because of both diffusion and erosion mechanisms, whereas drug release mechanism at pH 6.8–7.4 was because of Fickian diffusion.

Conclusion

The magnetic Alg beads are produced by simple ionic gelation and do not require detailed chemical synthesis. In this study, Alg–CS beads containing magnetic nanoparticles and ABZ were prepared in an attempt to obtain pH-sensitive magnetic hydrogel. The results showed that the beads possess excellent pH sensitivity in SR and superparamagnetic property as well as fast magnetic response, which indicated that the potential applications of these beads as a magnetic targeting system in the gastrointestinal tract.

Acknowledgments

This study was supported by the Lanzhou Foundation for Plan of Science and Technology, China (Grant No: 2009-1-55).

Declaration of interest

The authors report no conflicts of interest. The authors alone are responsible for the content and writing of this paper.

References

1. Seckin H, Yagmurlu B, Yigitkanli K, Kars HZ. (2008). Metabolic changes during successful medical therapy for brain hydatid cyst: Case report. Surg Neurol, 70:186–9.
2. Karadede A, Alyan O, Sucu M, Karahan Z. (2008). Coronary narrowing secondary to compression by pericardial hydatid cyst. Int J Cardiol, 123:204–7.
3. Li P, Zhang JP, Wang AQ. (2007). A Novel N-Succinyl chitosan-graft-polyacrylamide/attapulgite composite hydrogel prepared through inverse suspension polymerization. Macromol Mater Eng, 292:962–9.
4. Markoski MM, Trindade ES, Cabrera G, Laschuk A, Galanti N, Zaha A, et al. (2006). Praziquantel and albendazole damaging action on in vitro developing Mesocestoides corti (Platyhelminthes: Cestoda). Parasitol Int, 55:51–61.
5. Dayan AD. (2003). Albendazole, mebendazole and praziquantel. Review of nonclinical toxicity and pharmacokinetics. Acta Trop, 86:141–59.
6. Ramírez T, Eastmond DA, Herrera LA. (2007). Non-disjunction events induced by albendazole in human cells. Mutat Res, 626:191–5.
7. Rivera JC, Yepez-Mulia L, Hernandez-Campos A, Moreno-Esparza R, Castillo R, Navarrete-Vazquez G, et al. (2007). Biopharmaceutic evaluation of novel anthelmintic (1*H*-benzimidazol-5(6)-yl)carboxamide derivatives. Int J Pharm, 343:159–65.
8. Xu XH, Zh SD. (2002). Studies on preparation and dissolution of albendazole solid dispersions. Chin Pharm J, 37:283–6.
9. Vogt M, Kunath K, Dressman JB. (2008). Dissolution improvement of four poorly water soluble drugs by cogrinding with commonly used excipients. Eur J Pharm Biopharm, 68:330–7.
10. Evrard B, Chiap P, DeTullio P, Ghalmi F, Piel G, Van Hees T, et al. (2002). Oral bioavailability in sheep of albendazole from a suspension and from a solution containing hydroxypropyl-b-cyclodextrin. J Control Release, 85:45–50.
11. Horiuchia A, Satoua T, Akaob N, Koikea K, Fujitab K, Nikaidoa T. (2005). The effect of free and polyethylene glycol–liposome-entrapped albendazole on larval mobility and number in Toxocara canis infected mice. Vet Parasitol, 129:83–7.
12. Liu TY, Hu SH, Liu KH, Liu DM, Chen SY. (2008). Study on controlled drug permeation of magnetic-sensitive ferrogels: Effect of Fe_3O_4 and PVA. J Control Release, 126:228–36.
13. Li GY, Huang KL, Jiang YR, Yang DL, Ding P. (2008). Preparation and characterization of Saccharomyces cerevisiae alcohol dehydrogenase immobilized on magnetic nanoparticles. Int J Biol Macromol, 42:405–12.
14. Shamim N, Hong L, Hidajat K, Uddin MS. (2007). Thermosensitive polymer coated nanomagnetic particles for separation of bio-molecules. Sep Purif Technol, 53:164–70.
15. Mulder WJ, Strijkers GJ, Van Tilborg GAF, Griffioen AW, Nicolay K. (2006). Lipid-based nanoparticles for contrast-enhanced MRI and molecular imaging. NMR Biomed, 19:142–64.
16. Mueller-Schulte D, Schmitz-Rode T. (2006). Thermoresponsive magnetic polymer particles as contactless controllable drug carriers. J Magn Magn Mater, 302:267–71.
17. Gupta AK, Gupta M. (2005). Synthesis and surface engineering of iron oxide nanoparticles for biomedical applications. Biomaterials, 26:3995–4021.
18. Yuan Q, Venkatasubramanian R, Hein S, Misra RDK. (2008). A stimulus-responsive magnetic nanoparticle drug carrier: Magnetite encapsulated by chitosan-grafted-copolymer. Acta Biomater, 4:1024–37.
19. Sahiner N. (2007). Hydrogel nanonetworks with functional core-shell structure. Eur Polym J, 43:1709–17.
20. Kulkarni RV, Sa B. (2008). Evaluation of ph-sensitivity and drug release characteristics of (polyacrylamide-*grafted*-xanthan)–carboxymethyl cellulose-based pH-sensitive interpenetrating network hydrogel beads. Drug Dev Ind Pharm, 3:1406–14.
21. Hu SH, Liu TY, Liu DM, Chen SY. (2007). Nano-ferrosponges for controlled drug release. J Control Release, 121:181–9.
22. Douglas K, Tabrizian M. (2005). Effect of experimental parameters on the formation of alginate–chitosan nanoparticles and evaluation of their potential application as DNA carrier. J Biomater Sci Polym Ed, 16:43–56.
23. Anal AK, Stevens WF. (2005). Chitosan–alginate multilayer beads for controlled release of ampicillin. Int J Pharm, 290:45–54.
24. Kofuji K, Ito T, Murata Y, Kawashima S. (2001). Biodegradation and drug release of chitosan gel beads in subcutaneous air pouches of mice. Biol Pharm Bull, 24:205–8.
25. Thanou M, Verhoef JC, Junginger HE. (2001). Oral drug absorption enhancement by chitosan and its derivatives. Adv Drug Deliv Rev, 52:117–26.
26. Tavakol M, Vasheghani-Farahani E, Dolatabadi-Farahani T, Hashemi-Najafabadi S. (2009). Sulfasalazine release from alginate-N, O-carboxymethyl chitosan gel beads coated by chitosan. Carbohydr Polym, 77:326–30.
27. Xu XQ, Shen H, Xu JR, Xie MQ, Li XJ. (2006). The colloidal stability and core-shell structure of magnetite nanoparticles coated with alginate. Appl Surf Sci, 253:2158–64.
28. Gutsche S, Krause M, Kranz H. (2008). Strategies to Overcome pH-dependent solubility of weakly basic drugs by using different types of alginates. Drug Dev Ind Pharm, 34: 1277–84.
29. Liu XT, Yu WT, Wang W, Xiong Y, Ma XJ, Yuan Q. (2008). Polyelectrolyte microcapsules prepared by alginate and chitosan for biomedical application. Prog Chem, 20:126–39.
30. Dai YN, Li P, Zhang JP, Wang AQ, Wei Q. (2008). A novel pH sensitive N-Succinyl chitosan/alginate hydrogel bead for nifedipine delivery. Biopharm Drug Dispos, 29:173–84.
31. Wu Y, Guo J, Yang WL, Wang CC, Fu SK. (2006). Preparation and characterization of chitosan-poly(acrylic acid)polymer magnetic microspheres. Polymer, 47:5287–94.
32. Pasparakis G, Bouropoulos N. (2006). Swelling studies and in vitro release of verapamil from calcium alginate and calcium alginate-chitosan beads. Int J Pharm, 323:34–42.
33. Li QZ, Hao YH, Gao XJ, Gao WX, Zhao B. (2007). The target of benzimidazole carbamate against cysticerci cellulosae. Agric Sci China, 6:1009–17.
34. Kılıc-arslan M, Baykara T. (2003). The effect of the drug/polymer ratio on the properties of the verapamil HCl loaded microspheres. Int J Pharm, 252:99–109.
35. Rocher V, Siaugue JM, Cabuil V, Bee A. (2008). Removal of organic dyes by magnetic alginate beads. Water Res, 42: 1290–8.
36. Shu XZ, Zhu KJ. (2002). The release behavior of brilliant blue from calcium–alginate gel beads coated by chitosan: the preparation method effect. Eur J Pharm Biopharm, 53: 193–201.
37. Dai YN, Li P, Zhang JP, Wang AQ, Wei Q. (2008). Swelling characteristics and drug delivery properties of nifedipine-loaded pH sensitive alginate–chitosan hydrogel beads. J Biomed Mater Res, 86B:493–500.
38. Sankalia MG, Mashru RC, Sankalia JM, Sutariya VB. (2007). Reversed chitosan-alginate polyelectrolyte complex for stability improvement of alpha-amylase: Optimization and physicochemical characterization. Eur J Pharm Biopharm, 65:215–32.
39. Chen SC, Wu YC, MiFL, Lin YH, Yu LC, Sung HW. (2004). A novel pH-sensitive hydrogel composed of N, O-carboxymethyl chitosan and alginate cross-linked by genipin for protein drug delivery. J Control Release, 96:285–300.
40. Agatonovic-Kustrin S, Glass BD, Mangan M, Smithson J. (2008). Analysing the crystal purity of mebendazole raw

material and its stability in a suspension formulation. Int J Pharm, 361:245–50.
41. Hoffman AS. (2002). Hydrogels for biomedical applications. Adv Drug Deliv Rev, 43:3–12.
42. Bajpai SK, Sharma S. (2004). Investigation of swelling/degradation behavior of alginate beads crosslinked with Ca^{2+} and Ba^{2+} ions. React Funct Polym, 59:129–40.
43. Takka S, Ocak OH, Acartürk F. (1998). Formulation and investigation of nicardipine HCl-alginate gel beads with factorial design-based studies. Eur J Pharm Biopharm, 6: 241–6.
44. Siepmann J, Peppas NA. (2001). Modeling of drug release from delivery systems based on hydroxypropyl methylcellulose (HPMC). Adv Drug Deliv Rev, 48:139–57.